BULLETIN OF THE EARTHQUAKE
RESEARCH INSTITUTE
Vol. 37 (1959), pp. 571-592

36. *Studies of the Thermal State of the Earth. The Third Paper: Terrestrial Heat Flow at Hitachi, Ibaraki Prefecture, Japan.**

By Ki-iti HÔRAI,

Graduate School, University of Tokyo.

(Read July 22 and Sept. 22, 1959.—Received Sept. 30, 1959.)

Summary

From 68 measurements of rock temperature made at various points in drifts of Hitachi copper mine, geothermal gradients at these places were determined. The thermal gradient was found to be 0.94×10^{-2} °*C/m* and 1.21×10^{-2} °*C/m* in the north and the south parts of the mine respectively. Thermal conductivity of 36 rock specimens collected from various parts of the mine was measured using the divided-bar method. Apparent thermal conductivities of the rocks at the two parts are $6.73\sim7.08\times10^{-3}$ *cal/cm sec* °*C* and $6.50\sim7.43\times10^{-3}$ *cal/cm sec* °*C*. The terrestrial heat flow from the interior to the surface of the earth was computed to be $0.63\sim0.67\times10^{-6}$ cal/*cm*^{2} *sec* for the north part and $0.78\sim0.90\times10^{-6}$ *cal/cm*^{2} *sec* for the south part. These values are a little smaller than those already found in Japan.

1. Introduction

Determinations of the terrestrial heat flow have recently been made at several places in Japan by the Earthquake Research Institute. Preliminary heat flow values have already been published in this bulletin[1]. The results which were obtained by the writer in the Hitachi mine and are described in this paper will form an additional datum for studying thermal conditions in Japan. In the present study, so many observations of underground temperature and measurements of thermal conductivity of rock samples are made, that the heat flow value computed therefrom will be fairly reliable. The study was made possible by the permission and help given by the Nihon Kogyo Co. which operates the Hitachi mine (Ibaraki Prefecture). The location and topographical and structural

* Communicated by T. Rikitake.

1) S. UYEDA, T. YUKUTAKE and I. TANAOKA, *Bull. Earthq. Res. Inst.*, **36** (1958), 251.

Fig. 1. Map of Japan indicating the locality of Hitachi. Other localities where thermal investigation has been carried out are also shown.

Fig. 2. Topographic map of Hitachi. Framed area was under investigation.

features of the mine are shown in Figs. 1～3. Rock temperature was measured at 68 points in the drifts as shown in Fig. 4 i)～ix) and Fig.

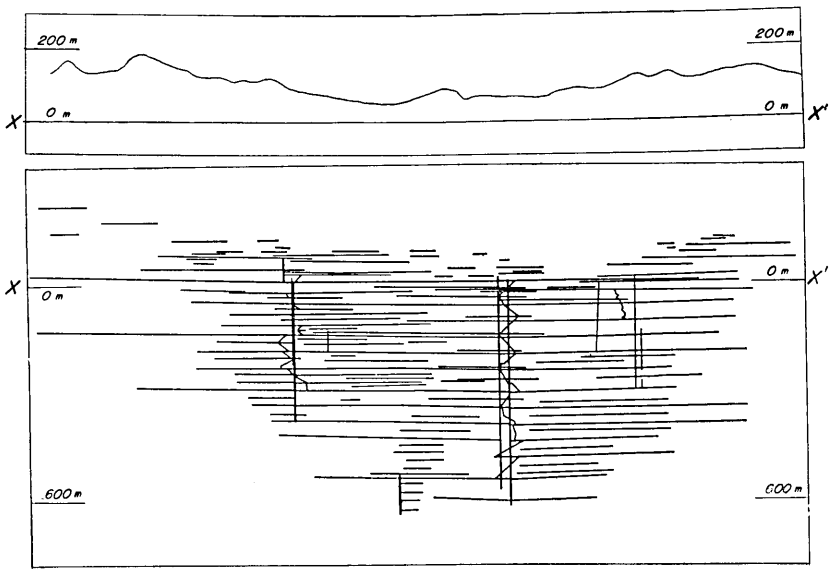

Fig. 3. Vertical section of the mine. The standard level (depth 0 *m*) is 349.6 *m* above sea level.

5. In the figure are also shown the points at which rock specimens were collected.

2. Thermal Conductivities of Rocks

36 rock specimens were collected from various points in the mine as illustrated in Fig. 4. Attempts were made to collect specimens of the rock species which are predominant in this area. Rocks collected were classified with the aid of a polarizing microscope. For opaque ore specimens a reflecting microscope was used for the purpose. Results of classification are given in Tables 2 and 3. It may be observed in Table 2 that the collected samples of rocks cover rock types well according to the abundance of mother rock types (*cf.* Fig. 12).

Each specimen of rocks was shaped for measurements as follows. A cylinder about 1 *inch* in diameter was cut out of a specimen by a diamond drill. Then it was cut into three or four disks by a diamond saw to obtain different thicknesses. We regard the specimens to be isotropic in macroscopic nature and do not take into account the

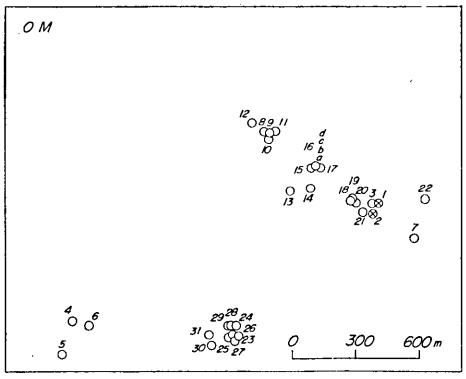

i) Depth 0 *m*.

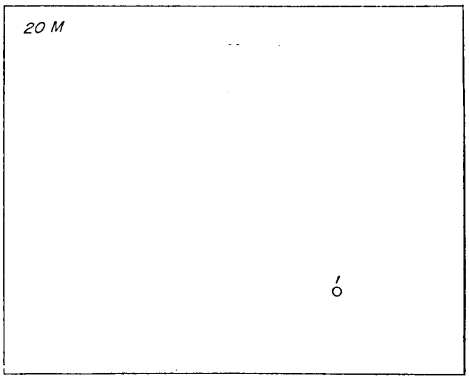

ii) Depth 20 *m*.

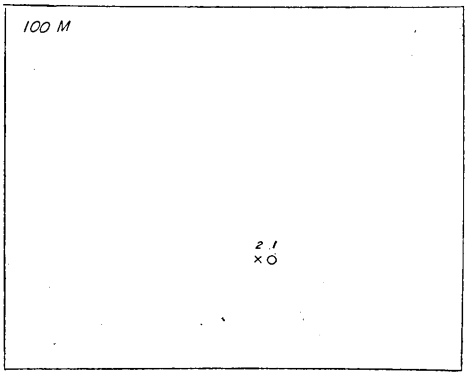

iii) Depth 100 *m*.

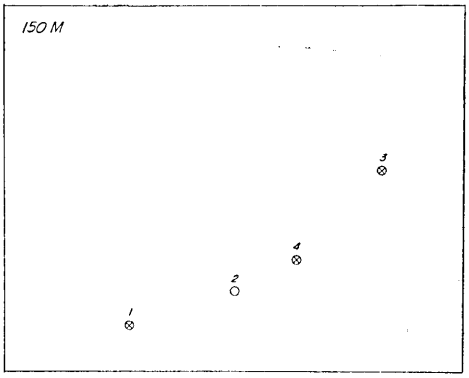

iv) Depth 150 *m*.

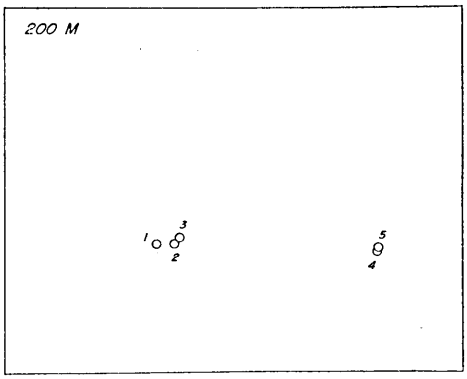

v) Depth 250 *m*.

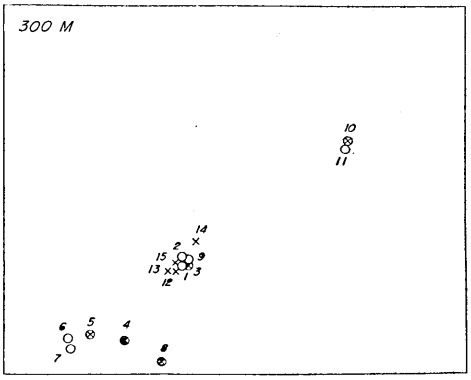

vi) Depth 300 *m*.

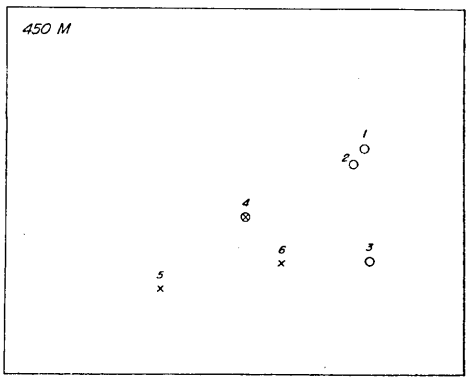

vii) Depth 450 *m*.

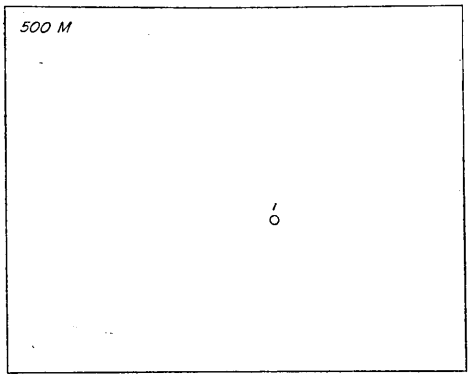

viii) Depth 500 *m*.

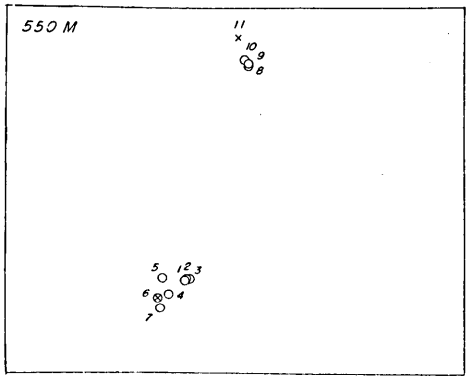

ix) Depth 550 *m*.

Fig. 4 i)~ix) Distribution of points where temperature measurements are made (marked by ○) and rock specimens are collected (marked by ×). The frame of the figures refers to that in Fig. 2.

Table 1. Distribution of points where temperature measurements are made.

Depth (*m*)	Number of points
0	31
20	1
100	1
150	4
250	5
300	11
450	4
500	1
550	10
Total	68

effect of orientation, structure and texture in the direction of cutting. Such an assumption is merely for convenience. In a few exceptional samples, rock specimens are apt to break into pieces along more or less definite breaking planes. In such cases the axis of the cylinder was taken perpendicular to the direction of the planes. The thickness of samples falls usually between 1 *mm* and 8 *mm*. Both the parallel surfaces of each disk were polished by corundum powder on an iron plate. Thicknesses and diameters of these

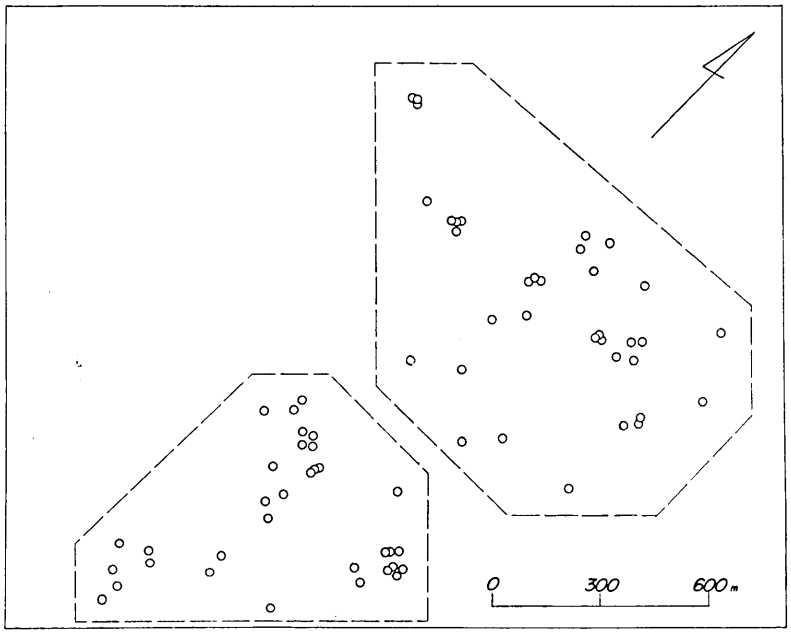

Fig. 5. Projection to the standard level of all the points where temperature measurements are made.

Table 2. Classification of rock specimens.

Rock type	Number of specimens
Hornblende biotite granodiorite	2
Mica granite Biotite muscovite granite Graphic two mica granite	4
Biotite amphibole schist Amphibole biotite schist Amphibole schist	15
Biotite quartz schist Amphibole quartz schist	3
Sericite schist	2
Biotite schist Biotite gneiss	5
Amphibole diabase Epidote schist	3
Massive chalcopyrite ore Massive cupriferous pyrite ore	2
Total	36

disks were measured by a micrometer, and their masses by a balance. The thickness within one and the same disked specimen varies usually less than 0.02 mm which is the accuracy of parallelism between the two surfaces. The diameter varies more remarkably. The mass was determined to an order of 0.001 gm.

Density. Density ρ was determined as a coefficient of linear relation $m=\rho v$ with the aid of the least square method, where m is the mass and v the volume of a specimen. Volume v is given as $v=\pi/4\cdot$

$\delta\phi^2$ where δ, ϕ are thickness and diameter of a disked specimen measured by a micrometer. Values of density thus determined are listed in the fifth column of Table 3.

Thermal conductivity. The divided-bar method was used for the measurement of thermal conductivity of rock samples. The apparatus used is the same as that which was described in the preliminary report[2]. The principle of measurement is briefly summarized as follows. As illustrated in Fig. 7, heat flows down from the upper brass bar to the lower through the specimen which is inserted between them and is carried away by cooling water. Under the state of steady flow of heat, we have relations such as

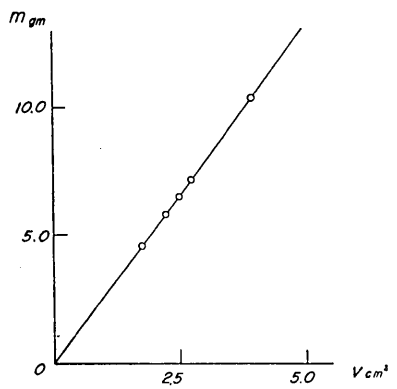

Fig. 6. An example of determination of density. Mass m versus volume v diagram is plotted for a set of specimens. Density ρ is determined as the slope $\rho=m/v$.

$$k_B \cdot p_B = k_R \cdot p_R \qquad (1)$$

$$T = L + p_R \cdot \delta = M \cdot p_B + p_R \cdot \delta \qquad (2)$$

where k_B and p_B are the thermal conductivity of the brass bar and the thermal gradient in it respectively, while k_R, p_R are those for the rock specimen. T is the temperature difference between D and E expressed as a sum of L which is the interfacial temperature drop and $p_R \cdot \delta$ the temperature drop in the specimen. δ is the thickness of the specimen. We assume that the interfacial drop is proportional to the thermal gradient in the brass bar and put $L=M \cdot p_B$, where M denotes the constant of proportionality. In our experiments, a disk-shaped specimen with thickness δ is inserted between the bars smeared with vaseline to improve the thermal contact at the interfaces and T and p_B are measured in the thermally steady state. The values of T/p_B are plotted against δ in

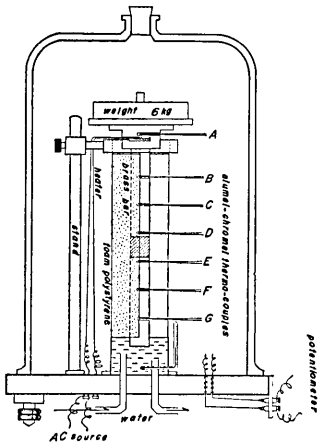

Fig. 7. Sketch of divided-bar apparatus.

2) S. UYEDA, T. YUKUTAKE and I. TANAOKA, *loc. cit.*

a diagram for a set of specimens. Then thermal conductivity is determined as follows. As derived from (1) and (2), the relation

$$T/p_B = M + \frac{k_B}{k_R} \cdot \delta \ , \qquad (3)$$

indicates that the slope α of a curve plotted in the T/p_B versus δ diagram is k_B/k_R, and k_R is given at once by

$$k_R = k_B/\alpha \ ,$$

if k_B is known. Diagrams of $T/p_B - \delta$ relation are given in Fig. 8 for all of our 36 specimens. Values of α are determined by fitting the relation $T/p_B = \alpha \cdot \delta + \beta$ to the diagrams with the aid of the least square method.

Calibration of divided-bar apparatus. To measure the conductivity of the brass bar k_B, crystalline quartz and fused quartz were used as standard substances. Two disked crystalline quartz specimens manufactured by the Quartz Crystal Co. of New Malden, Surrey, England were used. They are 2.128 *mm* and 4.143 *mm* in thickness respectively. They were cut so that heat flows in a direction normal to the optic axis and were assumed to have a thermal conductivity $k = 1/60.7 + 0.242\, t$ *cal/cm sec* °*C*[3], where t denotes temperature in centigrade. They were placed in place of rock specimens and k_B was determined by the process just reverse to what has been stated in the last section.

Special care was taken in conducting the experiments. First of all, thermometers B, C, D, E, F and G were calibrated and their characteristic curves were renewed. In the next place, as illustrated in Fig. 7, the brass bars were jacketed with *foam polystyrene*, an insulating material whose thermal conductivity is as low as about 0.00008 *cal/cm sec* °*C*. This material was used to reduce lateral heat losses.

The measurements gave $k_B = 0.219$ *cal/cm sec* °*C* at 40.3°*C* which agrees with an accuracy of 1% with the former result $k_B = 0.218$ *cal/cm sec* °*C* at 20°*C* which was obtained by Uyeda *et al.* who made use of pure iron as the standard[4].

Three fused quartz disks purchased from the Thermal Syndicate Ltd. of Wallsend-on-Tyne, England, were also used for calibration. The thermal conductivity of fused quartz is assumed to be $10^7 k = 31600 + 46\, t$

3) E. H. RATCLIFFE, *British Journal of Applied Physics*, **10** (1959), 22.

4) S. UYEDA, T. YUKUTAKE and I. TANAOKA, *loc. cit.*

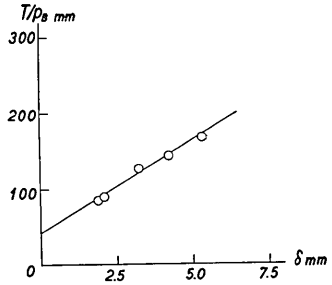

(I) α=24.03

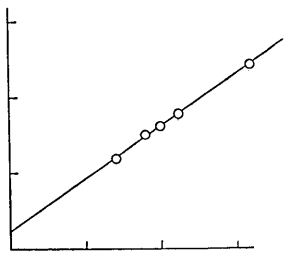

(II) α=28.04

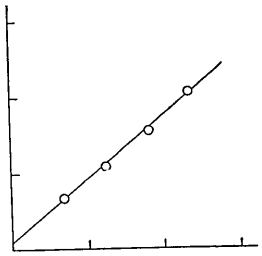

(III) α=33.06

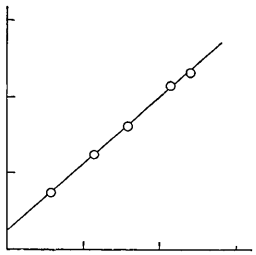

(IV) α=35.05

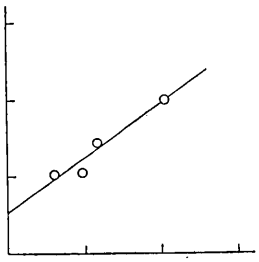

(V) α=28.82

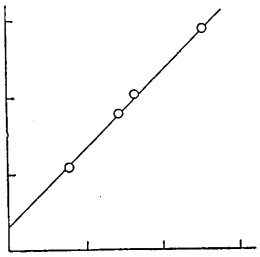

(VI) α=39.69

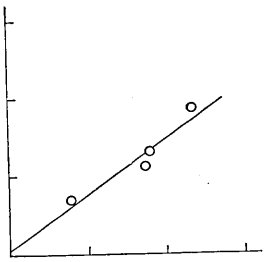

(VII) α=28.83

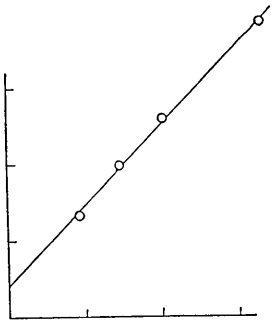

(VIII) α=41.89

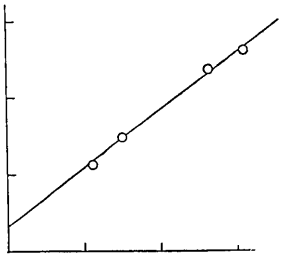

(IX) α=30.49

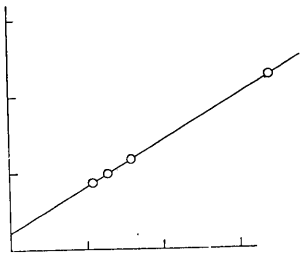

(X) α=24 01

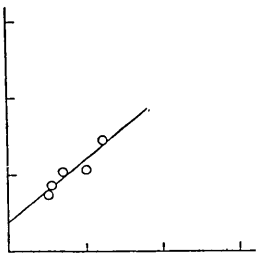

(XI) α=32.55

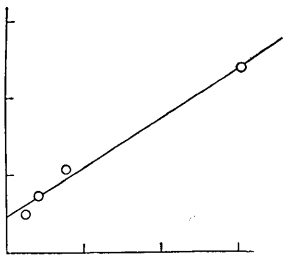

(XII) α=25.41

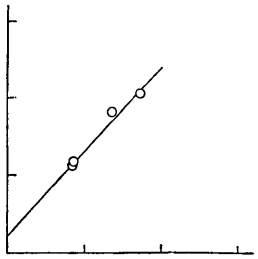

(XIII) α=43. 75

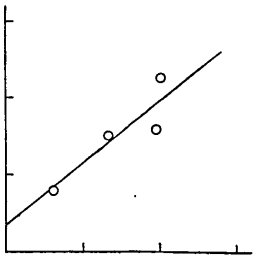

(XIV) α=31.95

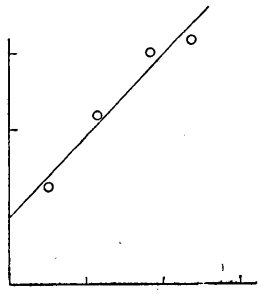

(XV) α=42.17

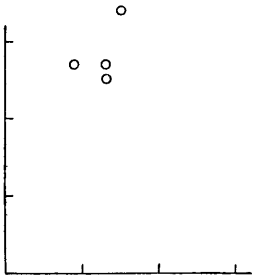

(XVI)

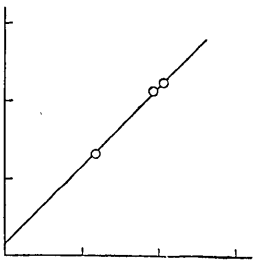

(XVII) α=40.66

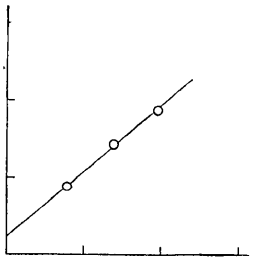

(XVIII) α=33.82

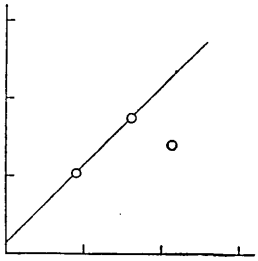

(XIX) α=40.10

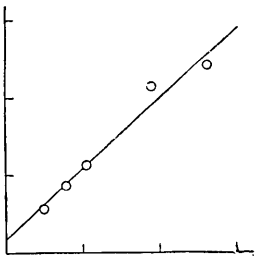

(XX) α=36.93

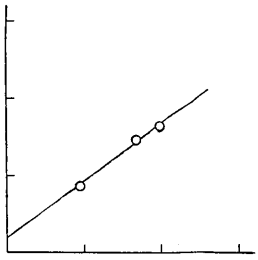

(XXI) α=29.51

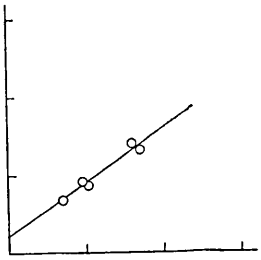

(XXII) α=27.76

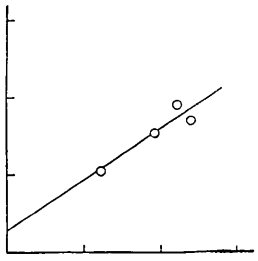

(XXIII) α=26.19

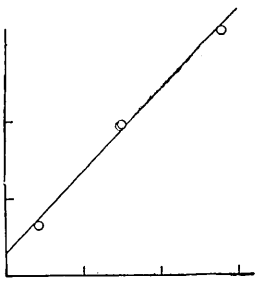

(XXIV) α=42.13

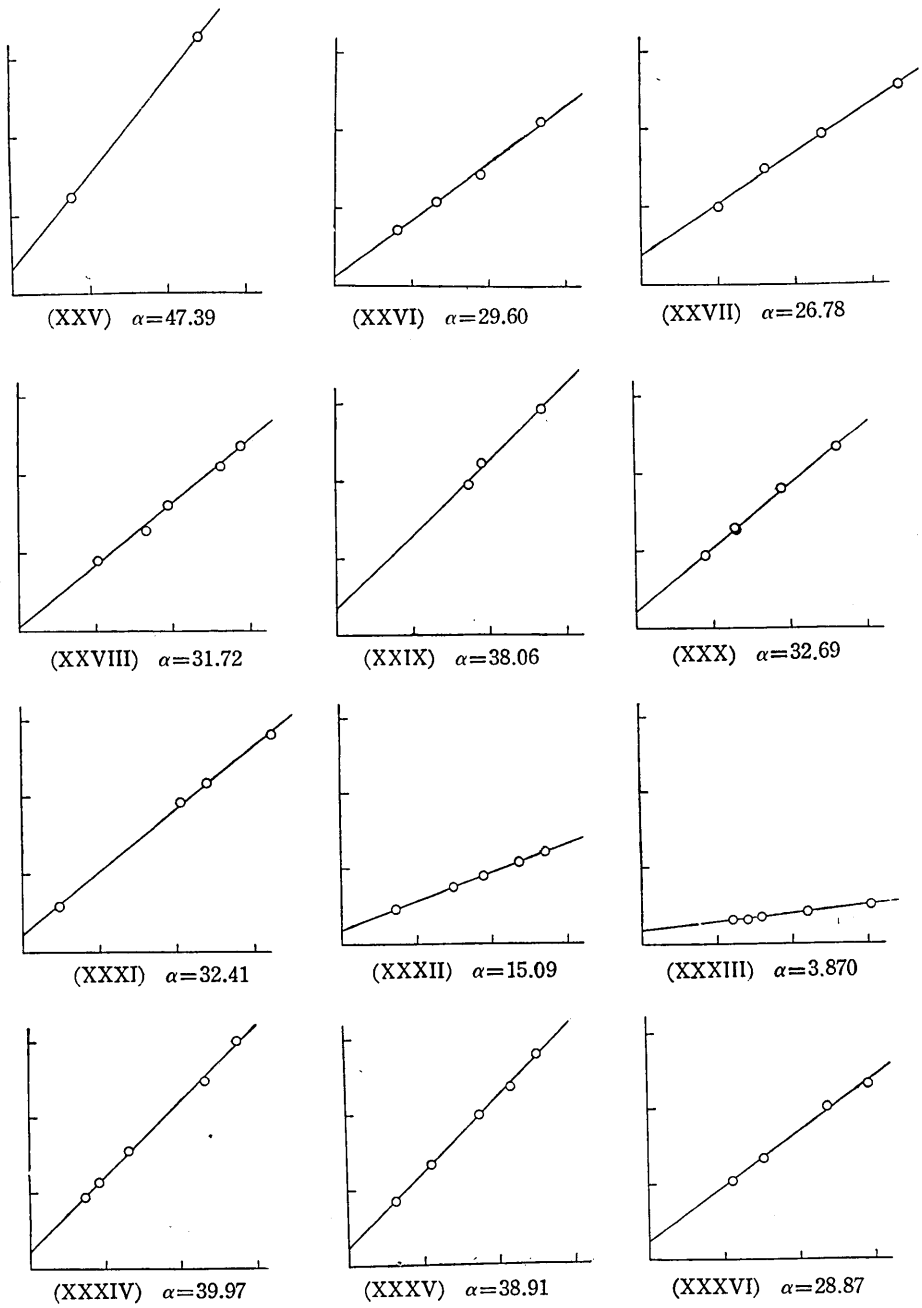

Fig. 8. T/p_B versus δ diagrams for all 36 rock specimens.
Unit: ordinate (T/p_B).....100 *mm*
abscissa (δ) .....2.5 *mm*

$-0.16\,t^2\,cal/cm\,sec\,°C$[5] where t again denotes temperature. The measurements gave $k_B=0.201\,cal/cm\,sec\,°C$ at 42.5 °C but this does not agree with that reduced from the experiments by use of crystalline specimens. According to microscope examinations, it was found that the fused

Table 3. Thermal conductivity of rock specimens.

Classification (*cf* Fig. 12)	Rock type	Specimen	Spot of collection	Density (gm/cm^3)	Thermal conductivity ($\times 10^{-3}$ *cal/cm sec °C*)	Mean temperature during measurement (°C)
A	Hornblende biotite granodiorite	HT XXX	550–11	2.73	6.70	35.0
		HT XXXI	550–11	2.75	6.76	37.5
B	Mica granite	HT II	0– 1	2.60	7.81	26.4
	Biotite muscovite granite	HT XXVI	550–11	2.62	7.40	37.5
	Graphic two mica granite	HT XXVII	550–11	2.58	8.18	35.1
		HT XXVIII	550–11	2.60	6.90	37.6
C, E	Biotite amphibole schist	HT III	0– 2	2.88	6.62	27.0
	Amphibole biotite schist	HT XI	300– 5	2.69	6.73	36.1
	Amphibole schist	HT V	100– 1	2.96	7.60	34.2
		HT VI	150– 1	2.86	5.52	34.2
		HT VIII	150– 4	2.86	5.23	33.8
		HT IX	300– 3	2.83	7.18	34.7
		HT XII	300– 8	2.75	8.62	34.9
		HT XIII	300–10	3.00	5.01	35.3
		HT XIV	300–10	2.97	6.85	35.1
		HT XVII	450– 4	2.92	5.39	37.1
		HT XVIII	450– 4	3.09	6.48	37.2
		HT XXI	450– 6	2.72	7.42	36.4
		HT XXIV	550– 6	2.92	5.20	38.7
		HT XXV	550– 6	2.88	4.62	37.0
		HT XXIX	550–11	2.85	5.75	37.1
D	Biotite quartz schist	HT XXII	500– 1	2.66	7.89	33.8
	Amphibole quartz schist	HT XXIII	500– 1	2.66	8.36	35.0
		HT X	300–14	2.69	9.12	34.5
F	Sericite schist	HT XIX	450– 5	2.68	5.46	37.8
		HT XX	450– 5	2.68	5.93	37.5
G	Biotite gneiss	HT I	0– 1	2.67	9.11	25.9
		HT IV	0– 2	2.78	6.25	33.0
		HT VII	150– 3	2.72	7.60	33.2
	Biotite schist	HT XV	300–12	2.72	5.19	39.0
		HT XVI	300–12	2.61		38.7
H	Amphibole diabase	HT XXXIV	300–15	2.96	5.48	38.1
		HT XXXV	300–14	2.97	5.63	39.3
	Epidote schist	HT XXXVI	350– 1	3.07	7.59	38.2
I	Massive chalcopyrite ore	HT XXXII	450– 7	4.05	14.51	35.7
	Massive cupriferous pyrite ore	HT XXXIII	300–13	4.68	56.59	33.5

5) E. H. RATCLIFFE, *loc. cit.*

quartz specimens have partially changed into crystalline state. It might be therefore concluded that the discrepancy between the results based on fused and crystalline quartz samples is likely to be caused by the impurity in fused quartz. Hence, the standard value is taken as $k_B = 0.219\ cal/cm\ sec\ °C$ throughout this paper.

As k_B was determined from the experiments mentioned above, k_R's are easily calculated. They are listed in the sixth column of Table 3.

3. Underground Temperature of the District

Measurement of rock temperature. To obtain true rock temperatures, it is necessary to put a thermometer in drill holes extending into regions which are free from the effect of ventilation or stagnation of air in drifts. Prior to actual measurements, we investigated the situation mathematically on a simple model, a brief description of which will be given below.

Suppose that a hole with a circular cross section and infinite length penetrates an infinite homogeneous material of uniform temperature and its temperature is suddenly raised or lowered by certain amount, 1 °C say, from the surrounding material and is maintained constant thereafter. How will the temperature outside the hole change with time? The question may be answered by solving the partial differential equation of conduction of heat in a cylindrical coordinate, which is

$$\frac{\partial T}{\partial t}=\kappa\left(\frac{\partial^2 T}{\partial r^2}+\frac{1}{r}\frac{\partial T}{\partial r}\right), \quad a\leq r\leq\infty\ , \tag{4}$$

under the conditions

$$\left.\begin{aligned} t=0 &: \quad T=0 \\ t>0 &: \quad T=1 \quad \text{at} \quad r=a \end{aligned}\right\}, \tag{5}$$

where t, r, a, κ denote time, radial distance referred to the axis of hole, the radius of the hole, thermal diffusivity of the material, respectively and T is the tempepature of material as a function of t and r.

An asymptotic solution of the equation, which is capable of numerical manipulation, is given in the form[6]

6) H. S. CARSLAW and J. C. JAEGER, *Conduction of Heat in Solids* (Oxford at the Clarendon Press, 1950), § 127.

$$T=\frac{a^{1/2}}{r^{1/2}}erfc\frac{r-a}{2\sqrt{\kappa t}}+\frac{(r-a)(\kappa t)^{1/2}}{4a^{1/2}r^{3/2}}ierfc\frac{r-a}{2\sqrt{\kappa t}}$$
$$+\frac{(9a^2-2ar-7r^2)\kappa t}{32a^{3/2}r^{5/2}}i^2erfc\frac{r-a}{2\sqrt{\kappa t}}+\cdots . \qquad (6)$$

The first term of it, which satisfies the imposed conditions (5) by itself, substituted into equation (4) yields for the left-hand side

$$\frac{\partial T}{\partial t}=\frac{2}{\sqrt{\pi}}\left\{\sqrt{\frac{a}{r}}\frac{r-a}{4\sqrt{\kappa}\,t^{3/2}}e^{-\frac{(r-a)^2}{4\kappa t}}\right\}, \qquad (7)$$

and for the right-hand side

$$\kappa\left(\frac{\partial^2 T}{\partial r^2}+\frac{1}{r}\frac{\partial T}{\partial r}\right)=\frac{2}{\sqrt{\pi}}\left\{\sqrt{\frac{a}{r}}\frac{r-a}{4\sqrt{\kappa}\,t^{3/2}}e^{-\frac{(r-a)^2}{4\kappa t}}\right\}$$
$$+\frac{\sqrt{a}\,\kappa}{4r^{5/2}}\left(1-erf\frac{r-a}{2\sqrt{\kappa t}}\right). \qquad (8)$$

For the case in which we are concerned ($t\geq 3\times 10^7\ sec$, $r\geq 10^2\ cm$, $\kappa\simeq 10^{-2}\ cm^2/sec$), the additional term in (8), $10^{-6}\ c.g.s.$ in order, compared to the first term of (6), $1\ c.g.s.$ in order, assures us that we can adopt

$$T=\sqrt{\frac{a}{r}}\,erfc\,\frac{r-a}{2\sqrt{\kappa t}}, \qquad (9)$$

as an approximate solution of the problem.

In virtue of the solution (9), the distance necessary for the temperature to fall by some extent, 10 and 1% say, can be calculated.

Table 4. Distance required to diminish the effect to 10% and to 1%. $\kappa=1.09\times 10^{-2}\ cm^2/sec$ ($k=5.3\times 10^{-3}\ cal/cm\ sec\ °C$, $c=0.18\ cal/gm\ °C$, $\rho=2.70\ gm/cm^3$) and $a=1\ m$ are assumed tentatively.

t	$r(T\leq 0.1)$	$r(T\leq 0.01)$
6 *months*	8m	14m
1 *year*	10	18
5 *years*	17	36
10 *years*	21	49
50 *years*	34	98
100 *years*	41	132

Some numerical examples are given for various time epochs as are shown in Table 4.

It is suggested from the above calculation, that we may measure temperatures at points of every 1 or 2 m along a drill hole to see how far the effect really extends. The results are shown in Fig. 9 in which a calculated value is also shown for comparison. Though a definite correspondence between observed and calculated results is not recognizable, the investigation assured us that insertion of thermometer as deep as 20 m in holes is practically sufficient for observing true rock temperature.

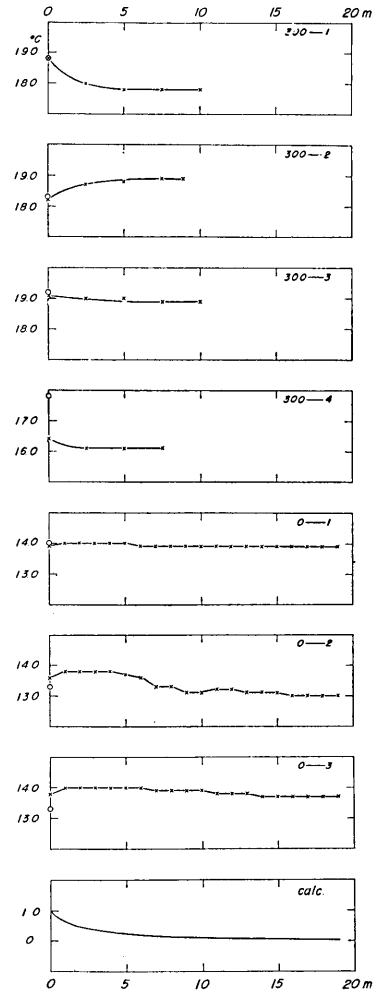

Fig. 9. Temperature variation in drill holes. Mark ○ denotes the temperature of the air in the drift near the opening of the hole. Calculated example is given for the case $t=1$ *year*, $\kappa=1.09\times10^{-2}$ *cm²/sec*, $a=1$ *m*.

Temperature measurements were made as follows. A thermister sealed in a pressure- and water-proof container was fixed to the top of an aluminium rod and was inserted into the hole and then another rod was joined to it which pushed the thermometer a little further. This process was repeated untill the thermometer reached the required position, for example 20 m distant from the opening, and the temperature was read by a portable potentiometer (connected to the thermometer with a water-proof lead wire) after the thermometer reached the state of thermal equilibrium. The thermister was calibrated in the laboratory before and after the measurements by a standard mercury-in-glass thermometer to the accuracy of 0.1°C.

Drill holes used are those which had been made for the purpose of searching for a vein of ore, whose diameters are about 1 *inch* and lengths extend usually some hundred meters. There were 835 such holes in the spring of 1959, but only 68 of them were usable for the measurements.

Results of measurements for all these 68 holes are tabulated in Table 5.

Table 5. Result of temperature measurement.

Depth	Date	No.	Length of insertion	Temperature	Note
0 *m*	1958 Nov. 15	1	19*m*	13.9 °*C*	
		2	19	13.0	
		3	19	13.7	
	1959 Mar. 13	1	20	14.1	
		2	20	13.3	
		3	20	12.8	
	12	4	20	12.0	
		5	20	12.7	
		6	20	12.5	
		7	3.9	21.4	
		8	20	12.3	
		9	10	12.4	
		10	20	12.3	
		11	20	12.4	
		12	20	11.5	
		13	20	12.6	
		14	20	12.6	
		15	20	12.3	
		16 a	20	12.2	
		16 b	30	12.2	
		16 c	40	12.2	
		16 d	50	12.2	
		17	20	12.3	
	13	18	20	12.5	
		19	20	12.7	
		20	15.3	12.7	
		21	9.2	12.7	
		22	20	12.2	
		23	20	12.3	
		24	20	12.5	
		25	20	12.5	
		26	18	12.3	
		27	20	12.4	
		28	20	12.4	
		29	17.3	12.8	
		30	20	12.9	
		31	20	13.7	
20 *m*	1959 Mar. 19	1	20	12.1	
100 *m*	1959 Mar. 19	1	3.3	14.2	
150 *m*	1959 Mar. 14	1	20	15.2	
		2	7.3	14.0	
		3	8	13.1	
		4	12.6	16.5	
250 *m*	1959 Mar. 19	1	20	15.1	
		2	11.3	18.0	
		3	16	21.8	
	20	4	15	23.4	
		5	20	24.6	

(to be continued)

Table 5. Result of temperature measurement. (continued)

Depth	Date	No.	Length of insertion	Temperature	Note
300 *m*	1958 Nov. 14	1	10	17.8	
		2	8.9	18.9	
		3	10	18.9	
		4	7.5	16.1	
	1959 Mar. 16	1	20	17.3	
		2	12	18.6	
		3	20	18.4	
		4	14	16.0	
		5	20	15.9	
		6	20	15.8	
		7	20	16.0	
		8	20	15.8	
		9	7	20.7	
		10	4.3	14.5	
		11	20	14.8	
450 *m*	1959 Mar. 17	1	20	16.4	
		2	20	16.5	
		3	20	17.2	
		4	3	16.7	
500 *m*	1959 Mar. 18	1	20	17.3	
550 *m*	1959 Mar. 18	1	20	19.3	
		2	20	19.3	
		3	20	19.2	
		4	20	19.4	
		5	20	19.3	
		6	20	19.2	
		7	20	19.3	
		8	20	17.8	
		9	20	18.0	
		10	20	17.9	

Temperature gradient. All the results of temperature measurements were projected to the vertical section showing the variation of subsurface temperature as illustrated in Fig. 10. Isothermal levels are

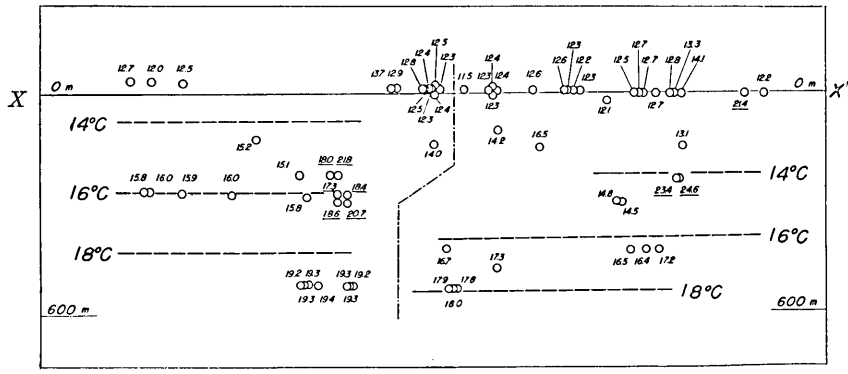

Fig. 10. Variation of underground isotherms projected to the vertical section X–X′.

found to be nearly horizontal showing that the geothermal heat flows nearly vertically in this region. In order to smooth out the isothermal curves, 9 points (marked by underlines) out of 68 are neglected because they are considered to be local anomalies due probably to the heat of oxidation. Difference of isothermal levels between the north and south parts becomes clear when it is represented by the avarage temperature gradients as can be seen in Fig. 11. The average temperature gradients were

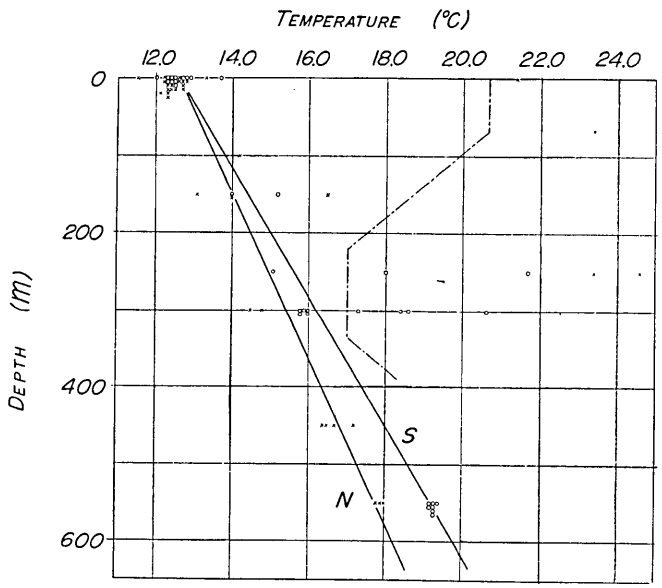

Fig. 11. Average temperature gradients for the north and south parts. Mark × is for the north part and ○ for the south part. The exceptional 9 points are bracketed by a chain line.

calculated using the least square method. It is $0.94°C/100\,m$ for the north part and $1.21°C/100\,m$ for the south part respectively.

4. Heat Flow Determination

In order to obtain the amount of heat flow in the north and south parts by calculating the product of the thermal gradient and the thermal conductivity, apparent thermal conductivities averaged through each part should be estimated. For that purpose we shall set a simple model and calculate the apparent conductivities from the conductivities of rock specimens. According to geological data accumulated so far, geological features are all alike whatever underground level we may take

as far as underground structures not deeper than several hundred meters are concerned. It is then possible to idealize the structure of the region under investigation to be composed of columns of different rock types in which heat flows to the direction parallel to the axis of columns. On this assumption the bulk thermal conductivity of a volume composed of many columns of different conductivity can be calculated in the following way. Let Q_i be the heat flow per unit time across a section of i'th column whose area of section is S_i and thermal conductivity is k_i. Then the relation $Q_i=S_i\cdot k_i(\Delta T/\Delta l)$ holds provided the temperature gradient $\Delta T/\Delta l$ is the same for all columns. The total flow of heat is given as $Q=\sum Q_i=\sum(S_ik_i/S)\cdot S(\Delta T/\Delta l)$, so that $k=\sum(S_i/S)k_i$ is the apparent thermal conductivity averaged through the volume, where $S=\sum S_i$.

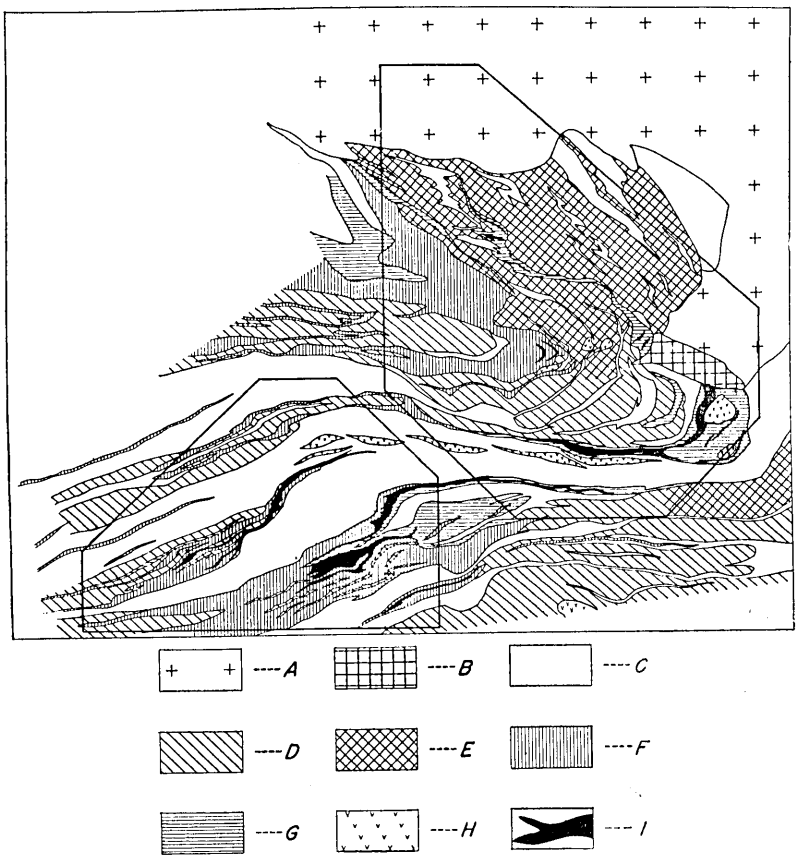

Fig. 12. Geological map of the area under investigation.

Planimetry was carried out on the geological map which was supplied by the courtesy of the Department of Geophysical Prospecting of the Hitachi Mine, Nihon Kogyo Co. (Fig. 12). The result is shown in Table 6. Combining it with the mean thermal conductivities of rocks, the apparent thermal conductivities are obtained, *i.e.* 7.08×10^{-3} *cal/cm sec* °*C*

Table 6. Result of planimetry and the mean thermal conductivity of rocks.

	North part (0.918 km^2)	South part (0.508 km^2)	Mean thermal conductivity ($\times10^{-3}$ *cal/cm sec* °*C*)
A	16.8 (17.0)		6.73
B	2.2 (2.2)		7.57
C, E	44.1 (44.6)	54.0 (55.8)	6.28
D	16.2 (16.4)	15.1 (15.6)	8.46
F	10.9 (11.0)	23.1 (23.9)	5.70
G	6.9 (7.0)	3.6 (3.7)	7.04
H	1.8 (1.8)	0.9 (0.9)	6.23
I	1.2	3.2	35.55
	100.1 (100.0)	99.9 (99.9)	

for the north part and 7.43×10^{-3} *cal/cm sec* °*C* for the south part respectively. As can be seen from Table 6, however, the mean conductivity of the ore is much larger than those of the rocks of ordinary types, so that its contribution to the apparent thermal conductivity is considerable though its area of exposure is only a minor fraction of the total. It is possible that the vein of the ore is far more exaggerated in the geological map than it really is. If we neglect the presence of the ore, the apparent conductivity becomes 6.73×10^{-3} *cal/cm sec* °*C* and 6.50×10^{-3} *cal/cm* sec °*C* respectively for the north and south parts. The true values are likely to lie between them, probably close to the latter ones.

The heat flow is given combining the results obtained above. It takes a value between $0.63\sim0.67\times10^{-6}$ *cal/cm² sec* for the north part and $0.78\sim0.90\times10^{-6}$ *cal/cm² sec* for the south part. It is not possible to determine the heat flow values because of the ambiguity in the thermal conductivities as has been discussed in detail in the last paragraph.

5. Discussion and Conclusion

By the investigations stated above, it is concluded that terrestrial heat flow at the Hitachi Mine takes a value between $0.63\sim0.67\times10^{-6}$

$cal/cm^2\,sec$ for the north part and $0.78\sim0.90\times10^{-6}\,cal/cm^2\,sec$ for the south part. They are definitely smaller than the values at Sasago reported in the first paper *i.e.* $2.06\times10^{-6}\,cal/cm^2\,sec$, at Yabase oil field[7] *i.e.* $2.01\times10^{-6}\,cal/cm^2\,sec$ or the global average $1.20\times10^{-6}\,cal/cm^2\,sec$. Contrary to the remarks stated in the first paper that physical and chemical processes in the crust accompanying orogenetic activity of Circum-Pacific Orogenetic Belts will cause greater heat flow in Japan, it is important that we have observed very low values of heat flow at Hitachi. At the moment, it is difficult to see the reason why such a small heat flow is observed here. Apart from further correction for possible effects of pressure, temperature and water content on the thermal conductivity of rock or effect of underground circulating water on the geothermal gradient, it will require some more laborious accumulation of data to clarify the question whether the results we obtained in this paper merely imply a local anomaly or are due to some large scale phenomena, for example thermal convection in the mantle as was suggested by Bullard *et al.*[8] and others[9] in the Pacific and the Atlantic Oceans.

6. Acknowledgement

This work was directed by Dr. T. Rikitake and the author thanks him for his kind guidance. He also wishes to express his thank to Professor C. Tsuboi for his encouragement. He is also grateful to Professor H. Tsuya for the classification of rock specimens and Mr. Okuno for the classification of ore specimens. He is indebted to Mr. T. Watanabe for the preparation of rock specimens used for the thermal conductivity measurements. He also acknowledges with thanks valuable discussion and help given by Dr. S. Uyeda, Dr. S. Akimoto, Mr. T. Yukutake and Mr. I. Tanaoka.

7) The thermal conductivity of rock specimens from Yabase oil field was measured by the author as shown in the following table. Combining these results with the geothermal gradient which has been already reported in the first paper, the heat flow is estimated at $2.01\times10^{-6}cal/cm^2\,sec$ there.

Formation	Rock type	Thermal conductivity
Funakawa (360~1030 *m*)	Shale	$3.43\times10^{-3}\,cal/cm\,sec\,°C$
Onagawa (1030~ *m*)	Shale	$5.47\times10^{-3}\,cal/cm\,sec\,°C$

8) E. C. BULLARD, A. E. MAXWELL and R. REVELLE, *Advances in Geophysics*, (Academic Press Inc.), **3** (1956), 153.

9) R. VON HERZEN, *Nature*, **183** (1959) *No.* 4665, 882.

Finally the author wishes to express his sincere thanks to the staff of the Hitachi Mine, Nihon Kogyo Co., especially to the members of the Department of Geophysical Prospecting, for without their whole-hearted cooperation and assistance this investigation could not have been completed. Professor Y. Shimomura and Mr. R. Imamura have kindly arranged the work. The author would like to extend his thanks to them.

---

36. 地球熱学 (第3報)
茨城県日立市に於ける地殻内熱流量

東京大学大学院
地球物理学専門課程 宝来帰一

茨城県日立市日立鉱山に於ける地下温度勾配及び岩石熱伝導率測定の結果，鉱山の北部及び南部の二地域で温度勾配はそれぞれ 0.94 °C/100 m，1.21 °C/100 m であること及び等温面がほぼ地表面に平行すなわち熱流の方向がほぼ地表面に垂直であることを見出した．又岩石熱伝導率測定値にもとづいて北部及び南部二地域の見かけの熱伝導率は $6.73\sim7.08\times10^{-3}$ cal/cm sec °C 及び $6.51\sim7.43\times10^{-3}$ cal/cm scc °C であると算定された．これによると，地殻内熱流量は北部に於て $0.63\sim0.67\times10^{-6}$ cal/cm² sec，南部に於て $0.79\sim0.90\times10^{-6}$ cal/cm² sec となるが，この値は第一報に報告された笹子トンネルに於ける結果 2.06×10^{-6} cal/cm² sec よりも低いのみならず世界の平均とされている 1.20×10^{-6} cal/cm² sec よりもなお低いようである．ここに求められた結果が，地殻内の局地的異常を表わすものか，或いは更に大規模な現象，中間層に於ける熱対流など，に関連あるものであるかどうかを追求するためには，更にこの種の研究の成果の集積をまたねばならない．
